THE ASTROPHYSICAL JOURNAL, 218:377–395, 1977 December 1

INTERSTELLAR BUBBLES. II. STRUCTURE AND EVOLUTION

ROBERT WEAVER, RICHARD MCCRAY, AND JOHN CASTOR
Department of Physics and Astrophysics, University of Colorado;
and Joint Institute for Laboratory Astrophysics, University of Colorado and National Bureau of Standards
AND
PAUL SHAPIRO* AND ROBERT MOORE
Center for Astrophysics, Harvard College Observatory and Smithsonian Astrophysical Observatory
Received 1977 March 21; accepted 1977 May 26

ABSTRACT

We present the detailed structure of the interaction of a strong stellar wind with the interstellar medium. First we give an adiabatic similarity solution, which is applicable at early times. Second, we derive a similarity solution, including the effects of thermal conduction between the hot ($T \approx 10^6$ K) interior and the cold shell of swept-up interstellar matter. We then modify this solution to include the effects of radiative energy losses. We calculate the evolution of an interstellar bubble, including the radiative losses. The quantitative results for the outer shell radius and velocity and the column density of highly ionized species such as O VI are within a factor 2 of the approximate results of Castor, McCray, and Weaver. The effect of stellar motion on the structure of a bubble, the hydrodynamic stability of the outer shell, and the observable properties of the hot region and the outer shell are discussed.

Subject headings: hydrodynamics — interstellar: matter — stars: winds

I. INTRODUCTION

In a previous paper (Castor, McCray, and Weaver 1975, hereafter Paper I), a theory was presented describing how an early-type star with a strong stellar wind blows a large cavity, or "bubble," in the ambient interstellar medium. The interior of the bubble is filled with hot ($T \gtrsim 10^6$ K) shocked stellar wind at low density and the swept-up interstellar gas is compressed into a thin spherical shell. We suggested that the O VI observed by the OAO-C *Copernicus* UV spectrometer in the spectra of such stars occurs in the interface, where thermal conduction dominates, between the hot interior of the bubble and the shell. In Paper I we made a number of approximations that permitted us to obtain simple analytic formulae for the structure and evolution of the bubble. We promised to present a more detailed theory and to discuss further observational consequences in a later paper; here we do so.

The plan of this paper is as follows. In § II we present solutions for the structure of an idealized model of adiabatic flow without thermal conduction. This model may be applicable to the early stages of the bubble and possibly to other systems, such as galactic winds. In § III we discuss the method of calculation used to find the detailed hydrodynamic structure of a bubble. In § IV we describe the details—density, temperature, ionization structure, and emission and absorption of radiation—of the interior of the bubble during the intermediate stage of evolution and compare the results with the approximate theory of Paper I. In § V we follow the evolution of the system into the late stage when radiative losses become comparable to the power of the stellar wind. We also describe approximately how the structure is modified by stellar motion. In § VI we describe the H I and H II regions surrounding the bubble. Finally, in § VII, we briefly summarize and add a few additional comments on observations.

* National Science Foundation Pre-doctoral Fellow.

II. EARLY STAGE

Most of the theory of this paper concerns the following idealized model. At time $t = 0$, an early-type star begins to blow a steady, spherically symmetric stellar wind with constant terminal velocity V_w and mass-loss rate dM_w/dt. The mechanical luminosity of L_w of the wind is therefore given by

$$L_w = \frac{1}{2}\frac{dM_w}{dt} V_w^2 . \quad (1)$$

This wind interacts with an ambient interstellar gas of uniform atomic density n_0 and given cosmic abundances, resulting in an expanding spherical system, which we shall call a bubble. Throughout its evolution, the dynamical system consists of four distinct zones. Starting from within, they are: (a) the hypersonic stellar wind; (b) a region of shocked stellar wind; (c) a shell of shocked interstellar gas; and (d) ambient interstellar gas. This structure is depicted schematically in Figure 1. In §§ IV and V we shall discuss some consequences of relaxing the above idealizations.

The evolutionary history of the bubble may be divided into three stages. At first, the bubble is expanding so fast that radiative losses in the gas do not

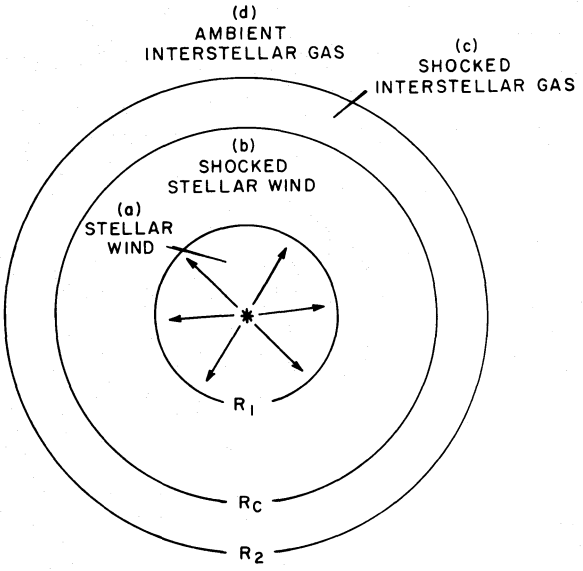

FIG. 1.—Schematic sketch indicating the regions and boundaries of the flow.

have time to affect any part of the system, and the dynamics of each region is described by adiabatic flow. In the second stage, discussed in § III, radiative losses cause the expanding shell of swept-up interstellar gas in region (c) to collapse into a thin shell; but region (b), the shocked stellar wind, still conserves energy. In the final stage, discussed in § V, the radiative losses also affect the dynamics of region (b).

The structure of the bubble during the first stage and the transition from the first stage to the second stage have been considered by Avedisova (1972) and by Falle (1975). They show that the first stage lasts a very short time; therefore, the structure during this first stage is of somewhat academic interest. However, we shall review the problem, since the above discussions are not complete, and since the hydrodynamical solutions we obtain may apply to a broader context than just the present model of a stellar wind interacting with interstellar gas.

We consider first region (c) of swept-up interstellar gas, whose outer boundary, at R_2, is a shock separating it from the ambient interstellar gas (d), and whose inner boundary, at R_c, is a contact discontinuity separating it from the shocked stellar wind (b). The structure of this region can be described by a similarity solution (Avedisova 1972). Our calculation parallels the theory of the adiabatic blast wave given by Taylor (1950); the only substantive difference in the case at hand is that the energy is fed into the system at a constant rate instead of in an initial blast.

Neglecting gravity and assuming that the flow is spherically symmetric, we find that the equations of motion and continuity are

$$\frac{\partial v}{\partial t} + v\frac{\partial v}{\partial r} + \frac{1}{\rho}\frac{\partial p}{\partial r} = 0\,, \tag{2}$$

and

$$\frac{\partial \rho}{\partial t} + v\frac{\partial \rho}{\partial r} + \rho\frac{\partial v}{\partial r} + 2\frac{\rho v}{r} = 0\,. \tag{3}$$

The equation of energy conservation for the adiabatic flow during this stage is

$$\frac{D}{Dt}(p\rho^{-\gamma}) = 0\,, \tag{4}$$

where $D/Dt \equiv \partial/\partial t + v\partial/\partial r$ and $\gamma = 5/3$.

As was shown in Paper I, the only dimensionless variable composed of L_w, ρ_0, r, and t can be written $\xi \equiv r/R_2(t)$ where

$$R_2(t) \equiv \alpha(L_w t^3/\rho_0)^{1/5}\,, \tag{5}$$

and α is a constant of order unity whose value remains to be determined. We define dimensionless functions of the self-similar flow by $v(r) \equiv V_2 U(\xi)$, $\rho(r) = \rho_0 G(\xi)$ and $p(r) \equiv \rho_0 V_2^2 P(\xi)$. With these definitions, equations (2)–(4) become

$$3(U - \xi)U' - 2U + 3P'/G = 0\,, \tag{6}$$

$$(U - \xi)G'/G + U' + 2U/\xi = 0\,, \tag{7}$$

and

$$3(U - \xi)P' - 3\gamma P(U - \xi)G'/G - 4P = 0\,, \tag{8}$$

where the primes denote differentiation with respect to ξ. As long as the expansion velocity V_2 of the bubble is much greater than the sound speed of the ambient interstellar gas, the shock at R_2 will be strong and the initial conditions needed to solve equations (6)–(8) are $G(1) = 4$, $U(1) = 3/4$, and $P(1) = 3/4$.

We have numerically integrated equations (6)–(7) inward to determine the self-similar structure of region (c); the results are shown in Figure 2. The remarkable property of this solution is that the density function $G(\xi)$ drops suddenly to zero at $\xi_c = 0.86$. This determines the location of the contact surface: $R_c = 0.86R_2$. At this point the pressure has the value $P(0.86) = 0.59$, and the velocity is given by $U(\xi_c) = 0.86$, or $v(R_c) = 0.86V_2$, as expected. This similarity solution was also obtained in a slightly different form by Avedisova (1972). However, the curves shown in Figure 1 there, particularly that of the pressure function, are not accurate.

We now consider the flow in region (b), whose outer boundary is the contact discontinuity at R_c and whose inner boundary is a shock at R_1. The assumption of a sharp discontinuity at R_1 is an idealization whose validity will be discussed in § III*b*. We shall see that the flow in region (b) is not self-similar (the ratio R_1/R_c varies with time). However, we can make a very good approximation that enables us to obtain analytic expressions for the flow variables there, namely, that region (b) is almost isobaric. To see this, consider first the flow near the inner shock at R_1. We have that $dR_1/dt \ll V_w$, since $dR_1/dt < V_2 \sim V_w(\rho_w/\rho_0)^{1/2} \ll V_w$. The sound speed is then $\sim V_w$, so that the time for a

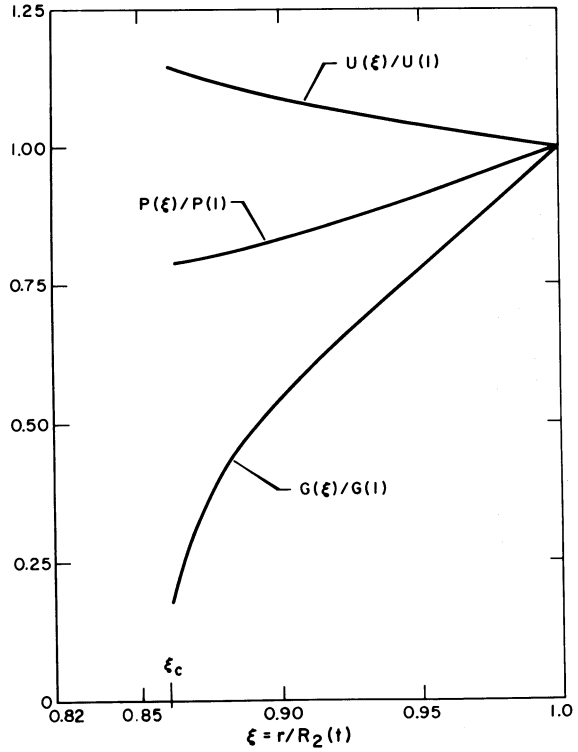

FIG. 2.—The similarity variables $U(\xi)$, $P(\xi)$, and $G(\xi)$ in region (c) for the adiabatic solution. The contact surface is at $\xi_c = 0.86$.

sound wave to cross region (b) is much less than the time t. Thus we may write the pressure of region (b) as a function only of time, $p(r, t) = p(t) = p(R_c)$, for $R_1 \leq r \leq R_c$. As a result, the adiabatic law and the continuity equation give

$$\frac{1}{\rho}\frac{D\rho}{Dt} = -\frac{1}{r^2}\frac{\partial}{\partial r}(r^2 v) = -\frac{12}{25t}. \quad (9)$$

An integration of equation (9) yields

$$v(r, t) = \frac{f(t)}{r^2} + \frac{4}{25}\frac{r}{t}. \quad (10)$$

The function $f(t)$ is determined by the boundary conditions on $v(r)$ at $r = R_c$. At R_c, $v(R_c) = 3R_c/5t$. Thus,

$$v(r, t) = \frac{11}{25}\frac{R_c^2}{r^2 t} + \frac{4}{25}\frac{r}{t}, \quad R_1 \leq r \leq R_c. \quad (11)$$

The Rankine-Hugoniot conditions at the inner shock give

$$v(R_1^+) = \frac{V_w}{4}, \quad \rho(R_1^+) = \frac{4dM_w/dt}{4\pi R_1^2 V_w},$$

$$p(R_1^+) = \frac{3}{4}\frac{V_w dM_w/dt}{4\pi R_1^2}.$$

In the region $R_1 \leq r \ll R_c$, the flow is nearly steady, and we can apply the adiabatic solar wind theory (see Holzer and Axford 1970), with $\gamma = 5/3$ and neglecting gravity. The appropriate subsonic solution is determined by the values above for v, ρ, and p at R_1^+. This solution gives the following relations for $R_1 \ll r \ll R_c$:

$$v \sim \frac{V_w}{4}\left(\frac{15}{16}\right)^{3/2}\frac{R_1^2}{r^2}, \quad \rho \sim \frac{4dM_w/dt}{4\pi R_1^2 V_w}\left(\frac{16}{15}\right)^{3/2},$$

$$p \sim \frac{3}{4}\frac{V_w dM_w/dt}{4\pi R_1^2}\left(\frac{16}{15}\right)^{5/2}.$$

The expression for v must match equation (11) when the second term in the latter is negligible. This implies

$$R_1 = \left(\frac{44}{25}\right)^{1/2}\left(\frac{16}{15}\right)^{3/4}\frac{R_c^{3/2}}{(V_w t)^{1/2}}$$

$$= 0.90\alpha^{3/2}\left(\frac{1}{\rho_0}\frac{dM_w}{dt}\right)^{3/10} V_w^{1/10} t^{2/5}. \quad (12)$$

Substituting for R_1 yields p for $R_1 \ll r \leq R_c$:

$$p(t) = \frac{5}{22\pi(0.86\alpha)^3}(L_w^2\rho_0^3)^{1/5} t^{-4/5}. \quad (13)$$

Comparing this expression with $p(R_c)$ shows that $\alpha = 0.88$.

A simple check on energy balance shows that these results are self-consistent. In region (b) the kinetic energy is negligible and the internal energy is

$$E_b = \tfrac{3}{2}[\tfrac{4}{3}\pi(R_c^3 - R_1^3)]p(t)$$

$$\approx 2\pi R_c^3 p(t) = \tfrac{5}{11}L_w t. \quad (14)$$

In region (c) the total energy E_c is just the work done up to the time t across the contact surface:

$$E_c = \int_0^t 4\pi R_c^2 v(R_c) p(t')dt' = \tfrac{6}{11}L_w t. \quad (15)$$

Thus, $E_b + E_c = L_w t$, which is the total energy released into the wind in time t. Numerical integration of appropriate functions of the similarity variables in region (c) shows further that 40.4% of E_c is kinetic energy, and 59.6% is thermal energy.

Avedisova (1972) derived an incorrect result $\alpha = 1.02$ from her similarity solution for region (c). As was pointed out by Falle (1975), this error is due to her assumption that the entire energy $L_w t$ was stored in region (c), in contrast to the correct result (eq. [15]). Our similarity solution for region (c) agrees in detail with the solution that Falle obtained by a hydrodynamical calculation.

The final function of interest is $\rho(r, t)$ for region (b). The streamlines satisfy equation (11), where $R_c \propto t^{3/5}$. An integration of equation (11) yields $r^3 = R_c^3 + Ct^{12/25}$. Since $R_c^3 \propto t^{45/25}$, all streamlines merge into the contact surface for large t. Note that C is negative for $r < R_c$, so these streamlines emerge from the origin at a finite time t_0, which depends on C. Let t' be

the time when a streamline crosses the inner shock. Then we have $r^3 = R_c^3(t) - R_c^3(t')(t/t')^{12/25}$, or $t' = t[1 - r^3/R_c^3(t)]^{25/33}$. Now, since $\rho \propto t^{-12/25}$ (from eq. [9]), we have $\rho(r, t) = \rho(R_1, t')(t'/t)^{12/25}$, where $\rho(R_1, t')$ is taken to be the result found above for when $R_1 \ll r \ll R_c$, i.e.,

$$\rho(R_1, t') = (25/11)t'(dM_w/dt)/4\pi R_c^3(t') .$$

Thus, we find

$$\rho(r, t) = 0.628\left[\left(\frac{dM_w}{dt}\right)^2 \rho_0^3 V_w^{-6}\right]^{1/5} t^{-4/5}\left[1 - \frac{r^3}{R_c^3(t)}\right]^{-8/33} . \quad (16)$$

Note that equation (16) assures that the total mass for $r \leq R_c$ is $t \times dM_w/dt$. Also, for $r \approx R_1 \ll R_c$, we have $\rho \approx$ constant, so the assumption of a quasi-steady flow was justified. The structure of region (b) given by equations (11) and (16) is also in agreement with the results obtained by Falle (1975).

The first stage of evolution terminates when the time scale for radiative cooling of the swept-up interstellar gas in region (c) becomes comparable with the age of the system. Estimates of this time scale by Avedisova (1972), by Falle (1975), and in Paper I are in fairly good agreement; the typical time scale is $\sim 2 \times 10^3$ yr for a stellar wind of power $L_w = 10^{36}$ ergs s^{-1} and ambient density $n_0 = 1$ cm^{-3}. Falle has investigated the collapse of region (c) in detail. He also shows that the structure of the bubble does not suffer the Rayleigh-Taylor instability during most of the evolution of the system, except possibly during the collapse of region (c). This is to be expected, since the expansion is always decelerating and the interior structure is stratified, with density increasing outward monotonically (see § V*c*).

III. INTERMEDIATE STAGE

a) Method of Calculation

During this stage the swept-up interstellar gas in region (c) has collapsed into a thin, almost isobaric shell. The inner part of the shell, an H II region with temperature $T \approx 10^4$ K (see § VI), is adjacent to the hot ($T > 10^6$ K) shocked stellar wind of region (b). The thermal conduction from region (b) to region (c) profoundly modifies the structure of the bubble during this stage. The conductive energy flux is balanced by a mechanical energy flux in the reverse direction associated with evaporation of mass from the cold region into the hot region and by radiative losses in the interface. As we shall show, the evaporated mass overwhelms the mass that came from the star and is the predominant source of mass for the hot region, yet the depletion of the mass of the cold shell is negligible.

The dynamics of the cold shell are easily described; the description is given in § II of Paper I, but it will be briefly repeated here. We let R_2 stand for the radius of the cold shell, which, when the shell is thin, can be the radius either of the outer shock, or of the interface with the hot region. At advanced times the shell thickness is not negligible (see § VI), and we let R_2 stand for the radius of the interface between the cold shell and the hot interior.

For the phase that will concern us in this section, R_1 is much less than R_2. (This will break down later.) Owing to the high temperature of the material between R_1 and R_2, the time for a sound wave to cross this region is small compared with the age, t, and therefore this entire region can be expected to be at a uniform pressure, p. Also, because this material is hot, the internal energy E contained within the region is much larger than the kinetic energy of the region. These facts allow us to find simple equations for the evolution of E and R_2 with time. The mass of the shell is given by $m_s = (4\pi/3)R_2^3\rho_0$. Since the volume within R_1 is negligible compared with that within R_2, E is related to p by

$$E = \frac{3}{2}\frac{4\pi}{3} R_2^3 p . \quad (17)$$

The momentum equation for the shell becomes

$$\frac{d}{dt}\left(\frac{4\pi}{3} R_2^3 \rho_0 \frac{dR_2}{dt}\right) = 4\pi R_2^2 p , \quad (18)$$

and the equation of energy balance for the hot region is

$$\frac{dE}{dt} = L_w - 4\pi R_2^2 p \frac{dR_2}{dt} . \quad (19)$$

As can be checked by direct substitution, the solution to equations (17)–(19) is given by

$$E = \tfrac{5}{11} L_w t , \quad (20)$$

$$R_2 = \left(\frac{250}{308\pi}\right)^{1/5} L_w^{1/5} \rho_0^{-1/5} t^{3/5} , \quad (21)$$

$$p = \frac{7}{(3850\pi)^{2/5}} L_w^{2/5} \rho_0^{3/5} t^{-4/5} . \quad (22)$$

Note that equation (21) has the same dimensional dependences as equation (5). However, the coefficient has changed from $\alpha = 0.88$ to $\alpha = 0.76$; this change is due to the collapse of region (c).

In the remainder of this section we shall be concerned with the properties of region (b), whose pressure is given by equation (22). We have found that the structure of this region can be described by a similarity solution, provided that the conductive and mechanical energy fluxes in this region dominate the radiative losses. We shall first derive this solution; later we shall incorporate the radiative losses as a modification to the basic solution.

We suppose that in the bubble interior the thermal conduction flux

$$F_c = -K\frac{\partial T}{\partial r} = -CT^{5/2}\frac{\partial T}{\partial r} \approx \frac{CT^{7/2}}{R_2}$$

is of the same order of magnitude as the mechanical energy flux

$$F_m = \frac{5}{2} pv \approx \frac{pR_2}{t} .$$

The coefficient of thermal conductivity is given by $K = CT^{5/2}$ (Spitzer 1962), where C is a weak function of temperature which we shall treat as a constant. (The effect of saturation of the conductive flux, discussed by Cowie and McKee 1977, will be considered below.) The flow speed, v, is of the same order as V_2 or R_2/t. In order that the two energy fluxes be comparable, T must be given by the following:

$$T \approx \left(\frac{pR_2^2}{tC}\right)^{2/7} = \frac{7^{2/7}5^{4/35}}{(154\pi)^{8/35}} \frac{(L_w)^{8/35}\rho_0^{2/35}}{C^{2/7}} t^{-6/35} .$$

Therefore we introduce the similarity variables ξ, τ, and $\mathscr{U}$, defined by

$$\xi = \frac{r}{R_2} , \tag{23}$$

$$\tau = \left(\frac{tC}{pR_2^2}\right)^{2/7} T , \tag{24}$$

$$\mathscr{U} = \frac{v}{V_2} = \frac{5}{3}\frac{vt}{R_2} . \tag{25}$$

We suppose that τ and $\mathscr{U}$ are functions of ξ alone, and independent of t. In the same way equation (7) was derived from equation (3), we then find

$$\frac{1}{\xi^2}\frac{d}{d\xi}(\xi^2\mathscr{U}) - \frac{\mathscr{U} - \xi}{\tau}\frac{d\tau}{d\xi} = \frac{22}{21} , \tag{26}$$

and from the energy equation, which with the addition of thermal conduction reads

$$\frac{D}{Dt}\left(\frac{3}{2}\frac{p}{\rho}\right) - \frac{p}{\rho^2}\frac{D\rho}{Dt} = \frac{1}{\rho r^2}\frac{\partial}{\partial r}\left(CT^{5/2}r^2\frac{\partial T}{\partial r}\right) , \tag{27}$$

we derive the nondimensional equation

$$\frac{1}{\xi^2}\frac{d}{d\xi}\left(\xi^2\tau^{5/2}\frac{d\tau}{d\xi}\right) - \frac{3}{2}\frac{\mathscr{U} - \xi}{\tau}\frac{d\tau}{d\xi} = \frac{13}{35} . \tag{28}$$

Equations (26) and (28) are the system we seek to solve in order to describe the hot region (b). Since the system is third-order in the space derivative, we need to impose three boundary conditions on the solution. These are: (A) The temperature tends to zero at $r = R_2$, i.e., $\tau \to 0$ as $\xi \to 1$. (B) The sum of the mechanical and conductive energy fluxes must tend at small radius to the value consistent with the power L_w supplied by the stellar wind. (C) The mass flux through a sphere of constant ξ must tend to zero as $\xi \to 0$. (The condition is tantamount to the assumption that the main contribution to the mass of region [b] is the evaporative flux.)

Condition B, the energy constraint, is readily imposed. Equations (26) and (28) can be combined to give

$$\frac{1}{\xi^2}\frac{d}{d\xi}\left[\xi^2\left(\frac{3}{2}\mathscr{U} - \tau^{5/2}\frac{d\tau}{d\xi}\right)\right] = \frac{6}{5} ,$$

which, when integrated, gives

$$\tfrac{3}{2}\mathscr{U} - \tau^{5/2}\frac{d\tau}{d\xi} = \tfrac{2}{5}\xi + \frac{C'}{\xi^2} , \tag{29}$$

where C' is a constant of integration. The value of C' follows from condition B. This arises from the fact that the total energy flux

$$F = \tfrac{5}{2}pv - CT^{5/2}\frac{\partial T}{\partial r}$$

leads to the expression

$$4\pi r^2 F = \tfrac{10}{11}L_w\xi^2\left(\tfrac{3}{2}\mathscr{U} - \tau^{5/2}\frac{d\tau}{d\xi}\right) = \tfrac{10}{11}L_w(\tfrac{2}{5}\xi^3 + C') ,$$

and, since condition B requires that the left side tend to L_w at small ξ, the value of C' must be 11/10. Therefore

$$\tfrac{3}{2}\mathscr{U} - \tau^{5/2}\frac{d\tau}{d\xi} = \tfrac{2}{5}\xi + \frac{11}{10\xi^2} . \tag{30}$$

Equation (30) can be used to eliminate $\mathscr{U}$ from equation (28) to give

$$\frac{\tau}{\xi^2}\frac{d}{d\xi}\left(\xi^2\tau^{3/2}\frac{d\tau}{d\xi}\right) - \frac{11}{10}\frac{1-\xi^3}{\xi^2}\frac{1}{\tau}\frac{d\tau}{d\xi} = \frac{13}{35} . \tag{31}$$

In order to impose condition A we look for a solution of equation (31) that tends to $\tau \sim A(1-\xi)^q$ as $\xi \to 1$, where q is a positive constant. We find that the only such value of q is 2/5, and that this form for τ satisfies the equation near $\xi = 1$ for all values of A. That is, we can assume

$$\tau \sim A(1-\xi)^{2/5} \quad \text{for } \xi \to 1 , \tag{32}$$

but A must be determined by the third boundary condition. A is related to the mass of the hot material. The rate at which mass evaporates from the shell into region (b) is given by ($p = \rho kT/\mu$)

$$\frac{dM_b}{dt} = \lim_{r \to R_2} 4\pi r^2\rho(\xi V_2 - v)$$

$$= \frac{4\pi R_2^3}{t}\frac{3}{5}\frac{\mu}{k}\left(\frac{tC}{R_2^2}\right)^{2/7} p^{5/7} \lim_{\xi \to 1}\left(\xi^2\frac{\xi - \mathscr{U}}{\tau}\right) .$$

The limit can be evaluated by using equations (30) and (32), with the result

$$\frac{dM_b}{dt} = \tfrac{12}{75}A^{5/2}\frac{4\pi R_2^3}{t}\frac{\mu}{k}\left(\frac{tC}{R_2^2}\right)^{2/7} p^{5/7} , \tag{33}$$

which, when integrated with respect to t, gives

$$M_b = \tfrac{28}{205} A^{5/2} 4\pi R_2^3 \frac{\mu}{k} \left(\frac{tC}{R_2^2}\right)^{2/7} p^{5/7} . \quad (34)$$

Condition C is a statement about the flux of mass through a sphere with a fixed value of ξ. That mass flux is proportional to $\xi^2(\xi - \mathscr{U})/\tau$, and so condition C takes the form

$$\lim_{\xi \to 0} \frac{\xi^2}{\tau} (\xi - \mathscr{U}) = 0 ,$$

which, in view of equation (30), can be written as

$$\lim_{\xi \to 0} \left[\frac{11}{15\tau} (\xi^3 - 1) - \tfrac{2}{3} \xi^2 \tau^{3/2} \frac{d\tau}{d\xi}\right] = 0 . \quad (35)$$

In order to apply condition (35) we look for a solution of equation (31) that is valid for small ξ. We suppose that for small ξ each term on the left side of that equation is large compared with unity, so that we may consider instead the equation

$$\frac{d}{d\xi}\left(\xi^2 \tau^{3/2} \frac{d\tau}{d\xi}\right) - \frac{11}{10\tau^2} \frac{d\tau}{d\xi} = 0 ,$$

which has the integral

$$\xi^2 \tau^{3/2} \frac{d\tau}{d\xi} + \frac{11}{10\tau} = C'' ,$$

in which C'' is another constant of integration. Upon comparing this integral with condition (35), we see that C'' must be zero. Another integration then gives

$$\tau = \left(\frac{77}{20\xi} + C'''\right)^{2/7} \approx \left(\frac{77}{20\xi}\right)^{2/7} , \quad (36)$$

with yet another constant of integration, C'''. The limiting form of τ for small ξ given by equation (36) can be used to evaluate the terms that were neglected in approximating equation (31), leading to the improved approximation

$$\frac{d}{d\xi}\left(\xi^2 \tau^{3/2} \frac{d\tau}{d\xi}\right) - \frac{11}{10\tau^2} \frac{d\tau}{d\xi} = \frac{24}{35} \left(\frac{20}{77}\right)^{2/7} \xi^{16/7} .$$

The first integral of this formula can be combined with equation (30) to give the behavior of the velocity for small ξ. It is

$$\mathscr{U} \sim \tfrac{28}{69} \xi .$$

In order to find the solution of equation (31) that has the behavior of equation (32) near $\xi = 1$ and the behavior of equation (36) for small ξ, we must solve the differential equation numerically. This is conveniently done by using equation (32) to initiate integrations inward from $\xi = 1$ for various values of A. Each integration leads to a value for the constant C'', and A is adjusted until $C'' = 0$. The value of A that is found is 1.646.

In Paper I, one of the main results was the formula for the temperature, $T = T_b(1 - \xi)^{2/5}$, in which T_b was given by equation (7) of that paper. A similar formula follows from equation (32) and the value that we have found for A. We combine these with equations (21), (22), and (24), and the numerical value 1.2×10^{-6} for the constant C in the Spitzer conductivity formula, and derive the numerical formula

$$T = 2.07 \times 10^6 L_{36}^{8/35} n_0^{2/35} t_6^{-6/35} (1 - \xi)^{2/5} \text{ K} , \quad (37)$$

where $L_{36} \equiv L_w/10^{36}$ ergs s^{-1} and $t_6 \equiv t/10^6$ yr. This differs from equation (7) of Paper I only in that the factor 1.98 of Paper I has become 2.07, a change of about 5%. The simple formula given in Paper I for column density of O VI ions is proportional to this coefficient to the power -1.5, so the column density is reduced by a factor of 0.9 on this account.

So far we have neglected the cooling of the hot gas by emission of radiation. This process causes a unit mass of gas to lose energy at the rate $n_e n \Lambda/\rho$, where Λ is a certain function of the electron temperature and ionization state of the gas. With the inclusion of radiative losses, the energy equation for region (b) becomes

$$\frac{D}{Dt}\left(\frac{3}{2}\frac{p}{\rho}\right) - \frac{p}{\rho^2}\frac{D\rho}{Dt} = \frac{1}{\rho r^2}\left(CT^{5/2} r^2 \frac{\partial T}{\partial r}\right) - \frac{n_e n \Lambda}{\rho} . \quad (38)$$

With the similarity solution above, the conduction term and the terms on the left side of equation (38) vary as $t^{-41/35}$, while the cooling term, if Λ can be regarded as a constant, varies as $t^{-22/35}$. So the cooling term grows in importance with time, and must eventually be considered. In practice, we have found that it must be included when the age exceeds about 10^5 years, if the central star is a typical luminous O star. When cooling is important, the main parameters of a bubble, i.e., $R_2(t)$, $V_2(t)$, and $E_b(t)$ must be allowed to deviate from their similarity solution values. The procedure we used to calculate the evolution of these parameters is discussed in § V. For our purposes here it is sufficient to say that we allowed for deviations from the similarity solution, due to radiation losses in region (b). Specifically, the instantaneous value of $d(\ln R_2)/d \ln t$ is used in place of the constant 3/5, the instantaneous value of $-d \ln p/d \ln t$ is used in place of 4/5, and an estimate is made of $(\partial \ln T/\partial \ln t)$ on the basis of previous detailed models. Let these three numbers be denoted by α, β, and δ, viz.,

$$\alpha = \frac{d \ln R_2}{d \ln t} , \quad (39)$$

$$\beta = -\frac{d \ln p}{d \ln t} , \quad (40)$$

$$\delta = \left(\frac{\partial \ln T}{\partial \ln t}\right)_\xi . \quad (41)$$

With these definitions, equations (3) and (38) become

$$\frac{1}{r^2}\frac{\partial}{\partial r}(r^2 v) - \left(v - \frac{\alpha r}{t}\right)\frac{1}{T}\frac{\partial T}{\partial r} = \frac{\beta + \delta}{t} \quad (42)$$

and

$$\frac{1}{pr^2}\frac{\partial}{\partial r}\left(CT^{5/2}r^2\frac{\partial T}{\partial r}\right) - \frac{5}{2}\left(v - \frac{\alpha r}{t}\right)\frac{1}{T}\frac{\partial T}{\partial r} - \frac{n_e n\Lambda}{p} = \frac{\beta + 2.5\delta}{t}. \quad (43)$$

These are analogous to equations (26) and (28). The boundary conditions are essentially the same:

A. $T \to 0$ as $r \to R_2$.

B. $v \to V_2$ as $r \to R_2$. (This is equivalent to the energy conditions used before.)

C. $v \to 0$ as $r \to 0$. (This is equivalent to eq. [35].)

The mass flux from the shell into the hot region is given by

$$\frac{dM_b}{dt} = \lim_{r \to R_2} 4\pi r^2 \frac{\mu p}{k}\frac{\alpha r/t - v}{T}.$$

This mass flux can be regarded as a parameter like A that must be adjusted in order to satisfy condition C. Equation (33) can be used as an initial estimate of dM_b/dt, which is then adjusted until the velocity found by numerical integration remains positive and less than $\alpha r/t$ at some chosen small radius. For each value of dM_b/dt, the integration of equations (42) and (43) can be initiated at a radius r slightly less than R_2 by using the relations

$$T = \left(\frac{25}{4}\frac{k}{\mu C}\frac{dM_b/dt}{4\pi R_2^2}\right)^{2/5}(R_2 - r)^{2/5}, \quad (44)$$

$$\frac{\partial T}{\partial r} = -\frac{2}{5}\frac{T}{R_2 - r}, \quad (45)$$

$$v = \frac{\alpha R_2}{t} - \frac{dM_b/dt}{4\pi R_2^2}\frac{kT}{\mu p}. \quad (46)$$

One of the most interesting aspects of the structures of the bubble is the set of column densities of ions that are responsible for absorption lines seen in the spectra of the central stars with the *Copernicus* ultraviolet telescope. For that reason, and also because the cooling function Λ depends on the state of ionization of the gas, we want to examine the time-dependent ionization of the gas as it evaporates and expands in the bubble interior. If $n_{i,j}$ is the number density of the jth stage of ionization of element number i, then we have the following ionization rate equations

$$\frac{\partial n_{i,j}}{\partial t} + \frac{1}{r^2}\frac{\partial}{\partial r}(r^2 v n_{i,j}) = n_e n_{i,j-1}C_{i,j-1} + n_e n_{i,j+1}\alpha_{i,j+1} - n_e(C_{i,j} + \alpha_{i,j})n_{i,j}. \quad (47)$$

The ionization and recombination processes we have included are those of the coronal approximation: collisional ionization (rate coefficient $C_{i,j}$) and radiative plus dielectronic recombination (rate coefficient $\alpha_{i,j}$). Ionization by the light of the central star is negligible in comparison with that due to electron collisions except in the region very near the cold shell where the temperature is too low to produce much collisional ionization. Similarly, ionization by cosmic rays and the X-ray background of the Galaxy can be neglected. One can easily check that ionization by UV and soft X-rays produced within the bubble is also negligible. We assume that the distributions of ionization stages within the bubble at different times are homologous, so that the ionization fractions $x_{i,j} = n_{i,j}/n_i$ are independent of time at a fixed value of r/R_2. This approximation should give acceptable results for the ionization fractions, since in the part of the bubble interior away from the cold shell the ionization state should tend to equilibrium, in which case the time-derivative term does not matter, and since near the cold shell the convective term in the equation will be much greater than the time-derivative term. The total density of element i, n_i, satisfies the continuity equation (3), so we find the following ordinary differential equation for the ionization fractions:

$$\left(v - \frac{\alpha r}{t}\right)\frac{dx_{i,j}}{dr} = n_e x_{i,j-1}C_{i,j-1} + n_e x_{i,j+1}\alpha_{i,j+1} - n_e(C_{i,j} + \alpha_{i,j})x_{i,j}. \quad (48)$$

The species that we have treated are H I–II, He I–III, C I–VII, N I–VIII, O I–IX, and Ne VI–XI. The collisional ionization rates used here, and the collisional excitation rates used for the calculation of Λ below, are given by Cox (1970) and Cox and Tucker (1969). The Cox and Tucker approximation for the ionization rates does not properly reflect the decrease in the ionization cross sections for high electron energies. As a result, for temperatures such that kT is much greater than the ionization potentials, the Cox and Tucker rates can significantly overestimate the true rates. The effects of our use of these rates, therefore, may have been to underestimate the degree to which the ions are out of ionization equilibrium. The dielectronic and radiative recombination rates were taken from Aldrovandi and Pequignot (1973). The cooling function Λ is given by

$$n_e n\Lambda = n_e \sum_i \sum_j n_{i,j}\left(\sum_k C'_{i,j,k}\chi_{i,j,k} + C_{i,j}\chi_{i,j}\right) + n_e n\Lambda_b, \quad (49)$$

where k labels excitation states of the ion i, j, $\chi_{i,j,k}$ is the excitation potential of the kth excited state above the ground state of that ion, $C_{i,j,k}'$ is the rate coefficient for excitation of that state from the ground state by electron collisions, $\chi_{i,j}$ is the ionization potential of that ion, and Λ_b is the bremsstrahlung cooling function. ($\chi_{i,j}$ and $\chi_{i,j,k}$ are taken from Cox 1970.) We have also added the approximate contribution to the total cooling function at $T \approx 10^6$ K due to Mg, Si, S, and Fe (see Shapiro and Moore 1976). Equation (49) expresses Λ in terms of the ionization

fractions and the temperature, and the ionization fractions are determined by equation (48). This cooling function is in turn used in equation (43) for the temperature structure, so that equations (42), (43), and (48) must all be integrated simultaneously.

b) Structure of the Inner Shock

In our work up to this point we have assumed that a shock front of negligible thickness exists at R_1, separating the free-streaming stellar wind from the hot, conduction-dominated material. Because of the very low density of the stellar wind, and its high velocity, we may question whether this is, in fact, the case. For the nominal conditions, $dM_w/dt = 10^{-6}\ M_\odot$ yr^{-1}, $n_0 = 1$ cm^{-3}, $t = 10^6$ yr, $V_w = 2000$ km s^{-1}, R_1 is 1.735×10^{19} cm $= 5.6$ pc. We would be worried about the validity of our solution if the shock thickness were greater than a few times 10^{18} cm. One estimate of the thickness is given by the stopping distances for the stellar wind electrons and ions in the hot region. Because of the high velocities, the stopping is done primarily by the electrons in the hot region. If the conditions are described by a density $n = 10^{-2}$ cm^{-3} and temperature $T = 10^6$ K, then the stopping distances calculated from the transport coefficients of Spitzer (1962) are 7.5×10^{14} cm for electrons, and 2.7×10^{18} cm for protons. In actuality, the shock front will very likely be of the collisionless type, in which binary particle interactions will be relatively unimportant. In the absence of a magnetic field, one might expect a turbulent electrostatic shock, as discussed by Tidman and Krall (1971). The shock thickness in this case is uncertain, but likely to be of the order of the wind speed divided by the proton plasma frequency. That distance is about 10^9 cm in this case. This thickness is certainly short enough to be neglected.

The shock structure that results from the collisionless shock is complicated by the fact that the shock transition affects the ions, but leaves the electron distribution function nearly unaltered. This is a result of the great mobility of the electrons, a property that is also responsible for the importance of conduction in the hot region. The solution we obtained for the temperature distribution in the small r region, which should apply just outside $r = R_1$, implies that the entire energy flux is carried by conduction. This is in contrast to the case discussed by, for example, Zel'dovich and Raizer (1967), in which conduction is negligible except in the shock front itself. Thus one should probably not think of the electrons as passing through a shock at all. Two other facts support this view. The first is that the mean thermal speed of the electrons in the conduction region is several times 10^8 cm s^{-1}, larger than the shock speed. The other fact is that the saturated conduction flux formula given by Cowie and McKee (1977) yields a value at R_1 that is nearly equal to the conduction flux demanded at that point by equation (36); the implication is that the electron velocity distribution is highly skewed in the outward direction. Thus the electron velocities are not randomized in direction upon passage through the shock, but only at a radius larger than R_1 where the conduction flux is not saturated.

Evidently the nature of the shock transition at R_1 is not simple, especially as it applies to the electron distribution function. Fortunately, the overall structure and evolution of the bubble do not depend on the details near R_1, because all of the power of the stellar wind must flow through this region into region (b), and this power alone determines the structure of the rest of the bubble. Furthermore, our predictions of observable properties of the bubble are quite insensitive to the model inadequacies in this region, owing to the fact that very little column density of any species is accumulated near R_1. Conversely, we may regret that the observations do not allow an opportunity to improve our understanding of collisionless shocks.

c) Validity of the Classical Conductivity Formula

Throughout our discussion up to now we have assumed that the energy flux due to thermal conduction is given by the classical formula of Spitzer (1962): $q_c = CT^{5/2}\nabla T$. Since this classical formula can under some circumstances predict a greater energy flux than can be carried by the electrons, we must verify that the thermal conduction is not "saturated." Cowie and McKee (1977) argue that the maximum allowable thermal energy flux is given by

$$q_s \approx 0.4(2kT_e/\pi m_e)^{1/2} n_e k T_e\ .$$

Their analysis includes the effect of the electric field that results from the slower diffusion rate of protons, as does the Spitzer formula. Cowie and McKee define a "saturation parameter" by $\sigma_s \equiv q_c/q_s$, and show that $\sigma_s \approx 4.6\lambda/L_T$, where λ is the mean free path of the thermal electrons (given by their eq. [3]) and $L_T \equiv T/|\nabla T|$.

We may estimate the importance of saturation in our theory by using the approximate formulae of Paper I for the structure and evolution of the bubble to obtain $\sigma_s \approx 0.1(T/T_b)^{1/2} L_{36}^{3/35} n_0^{-8/35} t_6^{-11/35}$. Thus we may conclude that in a typical bubble the thermal conduction is not saturated at the conduction front near R_c, where $T < T_b$, and that the Spitzer formula should be valid there. The conductive energy flux near R_c determines the rate of evaporation of gas into region (b), the O VI column density, and other observable properties of the bubble. Saturation of thermal conduction is likely to be significant near R_1, and this effect may cause the temperature and density structure near R_1 to be different from what we have calculated by using the Spitzer formula. As we have remarked, the structure of the shock there is uncertain anyway.

Another concern is that a magnetic field frozen in the shell (c) of swept-up interstellar gas may suppress the thermal conduction. But Cowie and McKee (1977, and private communication) have pointed out that this is not a significant effect, because any magnetic field should become combed in the radial direction as the gas diffuses from the shell into the low-density region (b).

IV. RESULTS—INTERIOR STRUCTURE OF A TYPICAL BUBBLE

In this section we present the results of a detailed calculation of the interior structure of a bubble. Let us consider an interstellar bubble of age $t = 10^6$ yr, surrounding a star of mass-loss rate $dM_w/dt = 10^{-6}$ $M_\odot$ yr^{-1} and wind velocity $V_w = 2000$ km s^{-1}, hence $L_w = 1.27 \times 10^{36}$ ergs s^{-1}, expanding into a medium of constant atomic density, $n_0 = 1$ cm^{-3} (henceforth we shall refer to these numerical values as a "typical bubble"). In the next section we shall discuss the time evolution of this bubble. The gross features of the temperature and density structure at $t = 10^6$ yr are shown in Figure 3. Working from the inside outward, one sees first region (a) of hypersonic stellar wind, whose density $n_w(r) \propto r^{-2}$ according to the continuity equation. This stellar wind encounters a shock at $R_1(t)$, some 6 pc from the central star. Beyond the shock is region (b) of hot ($T \gtrsim 10^6$ K) low-density shocked stellar wind that occupies most of the volume of the bubble. The gas in region (b) is an inefficient radiator, so the shock at $R_1(t)$ is not an isothermal one. However, thermal conduction carries energy away from the inner shock into region (b), so that the density discontinuity at $R_1(t)$ is greater than the value of 4 appropriate for an adiabatic shock, and the discontinuity is not sharp.

Region (b) is bounded by a thin shell (c) at $R_2(t) \approx 27$ pc of swept-up interstellar gas. This shell may be entirely H II, or it may also contain an outer layer of H I if the stellar radiation is insufficient to photoionize all the gas in the shell. The structure of this outer shell is described in more detail in § VI.

The interface between region (b) of shocked stellar wind and the shell (c) of swept-up interstellar gas is particularly interesting because there the temperature spans the range 10^5 K $< T < 10^6$ K, where highly ionized species such as O VI are the dominant ionization stages. The structure of this interface is determined by electron thermal conduction of heat from region (b) into the shell. Roughly 40% of the conductive heat flux is radiated away in the interface by collisional excitation of UV resonance lines such as O VI λ1035. The other 60% causes evaporation of gas from the shell, which diffuses into region (b) and mixes with the shocked stellar wind. In fact, the dominant source of mass in region (b), say, 35 $M_\odot$, is the interstellar gas evaporated from the shell (c) rather than the stellar wind itself. One can show that the saturation of thermal conductivity (see Cowie and McKee 1977) is not significant in this interface, although, as we have already mentioned, it is likely to be significant near the shock at R_1.

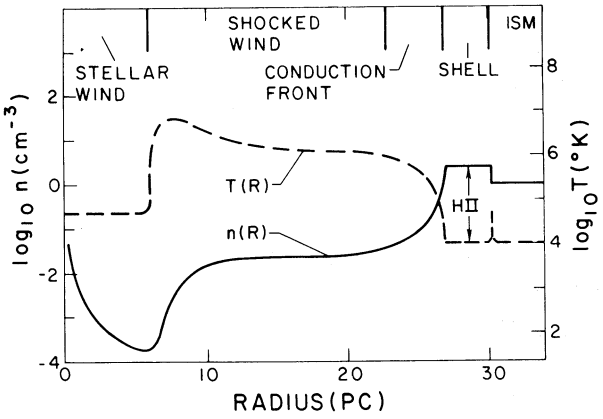

FIG. 3.—The large-scale features of the temperature and density structure of an interstellar bubble for which $L_w = 1.27 \times 10^{36}$ ergs s^{-1}, $n_0 = 1$ cm^{-3}, and $t = 10^6$ yr. ISM means ambient interstellar medium. For a typical O7 I star, the H II region would extend to $\sim 3\ R_2$.

In Paper I we calculated the column density of O VI and other ions through the conductive interface. To our surprise and delight, the theoretical column density of O VI turned out to be right in the range of column densities observed in the survey by Jenkins and Meloy (1974)! The theoretical result from Paper I is

$$N(\text{O VI}) \approx 3.4 \times 10^{16} X_0 n_0^{9/35} L_{36}^{1/35} t_6^{8/35} \text{ cm}^{-2}, \quad (50)$$

where X_0 is the fractional abundance of oxygen atoms. For example, equation (50) gives $N(\text{O VI}) \approx 1.5 \times 10^{13}$ cm^{-2} for typical values of stellar wind mass-loss rates and terminal velocities, a cosmic abundance of oxygen $X_0 = 4.4 \times 10^{-4}$, $n_0 = 1$ cm^{-3}, and $t = 10^6$ yr. It also implies that the observed column densities of O VI should not be correlated very well with the properties of the central star. The scaling law of $N(\text{O VI}) \propto L_w^{1/35}$ must break down for some later spectral types. This effect is discussed below in § V*b*, and in somewhat more detail by Weaver (1977).

In order to obtain the simple analytic description of the bubble in Paper I, we made three major approximations: first, we treated the conduction front in a plane-parallel approximation; second, we neglected the radiative losses in the conduction front; and third, we assumed that the ionization of trace elements in the conduction front was given by a coronal approximation, in which a local balance between collisional ionization and radiative recombination is assumed.

Each of these approximations has been removed in the present calculation. Figure 4 shows the temperature and density structure through the conduction front. The dominance of the electron thermal conduction is seen by the abrupt temperature rise from $T \approx 10^4$ to $T \approx 10^6$ K in a region only ~ 2 pc thick. The temperature gradient in the conduction front is slightly steeper than it was in our approximate model of Paper I, in which the radiative cooling term in the energy equation (38) was ignored. Including this term tends to increase $|dT/dr|$ at a given temperature.

The effect on N(O VI) of removing the three approximations is as follows. First, going from a plane-parallel description to a spherical description reduces the column density of O VI by about 10% (see eq. [37]). Removing the second approximation has a more significant effect. Since the inclusion of the radiative losses in the energy equation steepens the temperature gradient, the region where O VI predominates becomes

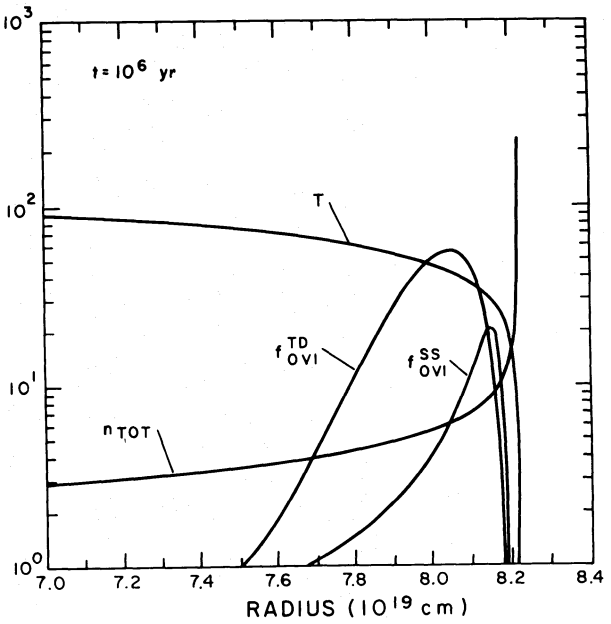

FIG. 4.—The detailed structure of the conduction front for the same model as in Fig. 3. The time-dependent and steady-state ionization fractions, $f_{O\,VI}^{TD}(r)$ and $f_{O\,VI}^{SS}(r)$, respectively, are shown. The units of the ordinate are, respectively, $T(10^4\ K)$, $n_{TOT}(10^{-2}\ cm^{-3})$, and $f_{O\,VI}^{TD}$, $f_{O\,VI}^{SS}(10^{-2})$.

more narrow. This reduces the column density of O VI by a further factor 0.5. However, these reductions are more than compensated by removing the third approximation of a steady-state ionization balance. When we calculate the ionization structure of trace elements in the conduction front by solving time-dependent rate equations, we find that the column density of O VI is increased by a factor 3.4 over the value obtained by using the steady-state assumption. This occurs because collisional ionization of O VI lags behind the temperature rise, with the result that the zone where the fractional abundance of O VI is large extends farther into the hot interior of the bubble. This effect can be seen on Figure 4, where we have also shown the steady-state and time-dependent fractions of O VI,

$$f_{O\,VI}(r) \equiv n(O^{+5}) \Big/ \sum_{i=0}^{8} n(O^{+i}) .$$

We have also calculated the theoretical profiles of the O VI absorption lines including the effects of thermal broadening and Doppler broadening owing to bulk motion of the gas. The region where $f_{O\,IV}(r)$ becomes large is physically narrow; thus there is a small change in the flow velocity across this region, and the optical depth $\tau_{O\,VI}(v)$ can be well represented by a Gaussian whose broadening is given by an effective temperature $T_{eff} \approx 4.5 \times 10^5$ K. The velocity of the line center v(O VI) relative to the central star is less than the outer shell velocity V_2 because it is formed in gas that is flowing inward relative to the shell. For this model we find $v(O\,VI) = 0.43V_2$, and typically v(O VI) is in the range $0.42V_2 < v(O\,VI) < 0.5V_2$ for other detailed models we have calculated.

We have also calculated the column densities of other highly ionized trace elements that may have observable UV absorption lines. The ratios of their column densities to those of O VI should be almost independent of the parameters of the system, and we find $\log N(X)/N(O\,VI) = -0.8$, -1.2, -2.0, and -1.5, respectively, for X = C IV, N V, Si IV, and S IV, assuming cosmic abundances $X_C = 3.3 \times 10^{-4}$, $X_N = 9.1 \times 10^{-5}$, $X_{Si} = 3.1 \times 10^{-5}$, and $X_S = 1.6 \times 10^{-5}$. (The approximate values quoted for Si and S in Paper I were wrong.)

The discrepancy between our theoretical value for $\log N(N\,V)/N(O\,VI) = -1.2$ and the value -1.6 found by York (1974) in the spectrum of λ Sco is less than before but still exists. We have no facile explanations for this discrepancy, but we would point out that the same discrepancy should be inherent in any hot gas model for O VI, be it circumstellar bubbles or supernova tunnels, unless the gas temperature happened to be at just the right value and did not span a range (see Shapiro and Moore 1976)—a highly unlikely situation, in our view.

The hot gas in the interior of the bubble should be a soft X-ray source. We have calculated the X-ray luminosity and spectrum of our model bubble by folding the spectral emissivity of the optically thin gas with the theoretical temperature and density structure shown in Figure 4. This spectral emissivity has been calculated from a revised version, to be published, of the code of Shapiro and Moore (1976), in which more atomic transitions and improved excitation and ionization rates have been included. The main result of this revision is that the total emissivity of soft X-rays is reduced by a factor of roughly 4 compared with that calculated by Tucker and Koren (1971). The resulting X-ray spectrum for $1\ Å \leq \lambda \leq 100\ Å$ is shown in Figure 5. This X-ray spectrum is calculated by assuming steady-state ionization balance. Since the collisional ionization of the various ions lags behind the temperature rise, ionization fractions for ions such as O VIII and N VII, which in the steady-state approximation are most abundant around $T \approx T_b \approx$ few times 10^6 K, will not be accurately calculated in the steady-state approximation. In general, we expect that $L_i^{SS} \gtrsim L_i^{TD}$, where SS(TD) refers to the steady-state (time-dependent) ionization balance, for those X-ray emitting ions i which in equilibrium are most abundant at $T \approx T_b$. Accordingly, the total soft X-ray emissivity in the TD case should be less than that in the SS case shown here. In order to examine just how sensitive the X-ray spectrum is to the steady-state approximation, we have calculated the luminosity of several X-ray lines by using the correct time-dependent ionization balance. We find, for example, that the luminosity of the O VIII hydrogen-like Lα line at $\lambda = 19.0$ Å is $L_{O\,VIII}^{TD} = 1.1 \times 10^{30}$ ergs s^{-1} and $L_{O\,VIII}^{SS} = 7.7 \times 10^{30}$ ergs s^{-1}, while the luminosity of the O VII helium-like line at $\lambda = 21.6$ Å is $L_{O\,VII}^{TD} = 2.4 \times 10^{32}$ ergs s^{-1} and $L_{O\,VII}^{SS} = 1.5 \times 10^{32}$ ergs s^{-1}.

Our calculated X-ray luminosity in the steady-state

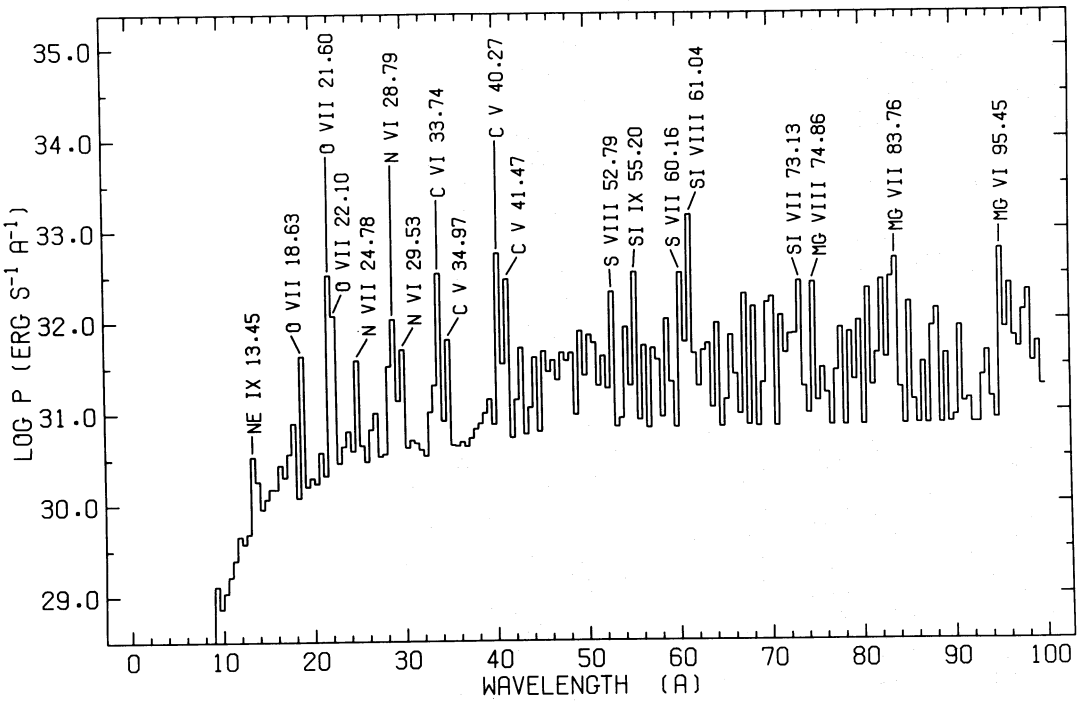

FIG. 5.—The X-ray spectrum of a bubble for 0.5 Å $\leq \lambda \leq$ 100 Å in 0.5 Å bins calculated from the detailed temperature and density structure of the same model as in Fig. 3 but assuming steady-state ionization balance. Some of the more important lines are labeled.

case, integrated over the 44–70 Å band, is $L_{44-70} = 2.2 \times 10^{33}$ ergs s^{-1} or roughly 10^{-3} times the total luminosity L_b of the bubble, which is expected to be comparable to the stellar wind luminosity L_w. (Most of L_b is emitted in the form of UV resonance lines such as O VI λ1035.) Therefore a typical bubble with $L_X \approx 10^{33}$ ergs s^{-1} is a very weak soft X-ray source compared with a typical supernova shell, for which $L_X \approx 10^{35}$ to 10^{36} ergs s^{-1}. Furthermore, the nearest stars of sufficiently early type to blow a bubble are the Orion stars, some 460 pc away. Some soft X-ray excess in the direction of Orion has been observed by the Wisconsin group (Burstein *et al.* 1977) and by the ANS group (den Boggende *et al.* 1977), and it is reasonable to assume that this excess is due to bubbles around these stars. However, the soft X-ray source in Orion is very faint compared with the Vela supernova remnant. Since the bubbles are intrinsically weak soft X-ray sources, and most are so distant that the intervening interstellar gas is opaque to soft X-rays, it is unlikely that they contribute significantly to the galactic soft X-ray background.

Another way that the hot interior of a bubble might be observed, in principle, is through optical or UV emission lines due to multiply ionized atoms. In order to see whether this is feasible, we calculate the differential emission measure through this hot interior region (b). Consider first looking at a bubble through the center of the apparent circle on the sky. The differential emission measure is then $d(\mathrm{EM})_0/dT = 2n^2/|dT/dr|$. Using the simple theory of Paper I for the temperature and density structure, we find that

$$\frac{d(\mathrm{EM})_0}{dT} = 5n_b^2 \frac{R_2}{T_b}\left(\frac{T_b}{T}\right)^{1/2} .$$

Thus, for a typical bubble with $t_b = 1$, for which $n_b \approx 10^{-2}$ cm^{-3}, $R_2 \approx 27$ pc, and $T_b = 2 \times 10^6$ K, we find that the total emission measure of the interior (10^4 K $< T < T_b$) is $(\mathrm{EM})_0 \approx 10^{-2}$ cm^{-6} pc. However, if one is looking for emission from some particular ion whose abundance peaks near R_2, there can be a significant limb-brightening effect. We have estimated that the resulting maximum enhancement factor of the emission measure is ~ 10. Emission measures of this magnitude may be observable with the Space Telescope.

V. EVOLUTION OF A TYPICAL INTERSTELLAR BUBBLE

a) Method of Calculation

The evolution of an interstellar bubble for typical conditions depends critically on the rate of energy loss due to radiation. If the radiative energy losses were negligible, the time dependence of the various parameters would be approximated very well by the formulae of Paper I. Here we summarize the main results given in that paper. The expansion of the outer shell was given by

$$R_2(t) = 27 n_0^{-1/5} L_{36}^{1/5} t_6^{3/5} \text{ pc} , \qquad (51)$$

from which one may readily derive the expansion velocity

$$V_2(t) = 16 n_0^{-1/5} L_{36}^{1/5} t_6^{-2/5} \text{ km s}^{-1} . \qquad (52)$$

Furthermore, since the radius, R_1, of the inner shock is determined by the balance between the ram pressure of the stellar wind and the internal energy density of region (b), the rate at which energy escapes region (b) crucially affects the volume of region (b). From the simple formula of Paper I, $L_b \propto t^{16/35}$, one might expect the radiative losses to continue to increase with time until $L_b > L_w$. If so, the energy, and hence the pressure of region (b), would drop, causing the inner shock to accelerate out. Region (b) would then collapse with $R_1 \approx R_2$, and the stellar wind would collide directly with the outer shell. The O VI column density would vanish, and the shell would then expand according to the law $R_{\rm shell}(t) \propto t^{1/2}$ given by Steigman, Strittmatter, and Williams (1975). However, if L_b remains less than L_w, the energy of region (b) would continue to increase for the duration of the stellar wind. We have found that $L_b \approx L_w$, so the assumption $L_b \approx 0$ must be removed. In this section we describe the method we used in order to follow the approach of L_b to L_w and the consequent deviation from similarity due to the radiative losses.

In order to determine the evolution of an interstellar bubble, allowing for radiative losses, we must modify equations (17), (18), and (19) to include the time variation of $R_1(t)$ and the radiative cooling. Thus the internal energy of region (b) is now

$$E_b = 2\pi p(R_2^3 - R_1^3) . \tag{53}$$

The pressure specified by equation (53) is then used to modify the momentum equation for the shell to obtain

$$\frac{d}{dt}\left(\frac{4\pi\rho_0}{3} R_2^3 \frac{dR_2}{dt}\right) = 4\pi R_2^2(p - p_{\rm II}) \tag{54}$$

where $p_{\rm II}$ is the pressure in the H II region outside the shell. This pressure is included until the H II region is trapped by the shell (see § VI). Pressure balance at R_1 yields:

$$R_1 = \left[\frac{L_w}{V_w E_b}(R_2^3 - R_1^3)\right]^{1/2} . \tag{55}$$

When cooling of region (b) is not negligible, L_b must also be included in the equation for the evolution of the total energy $E_b(t)$:

$$\frac{dE_b}{dt} = L_w - 4\pi R_2^2 p \frac{dR_2}{dt} - L_b . \tag{56}$$

The luminosity L_b is given by

$$L_b = \int_{R_1}^{R_2} n_e n \Lambda 4\pi r^2 dr , \tag{57}$$

and can be evaluated only when the temperature structure of the conduction front is known.

In principle one could solve the evolutionary equations (54), (55), and (56) by calculating $L_b(t)$ at each instant of time from a detailed structural model according to the method described in § III. However, this procedure is prohibitively expensive. Therefore we have derived an alternative procedure which consists of deriving an approximate formula for $L_b(t)$ and of using that formula to close the system of evolutionary equations.

We find that the time development of $L_b(t)$ can be estimated from equation (57) in the following manner. From equation (37) we have

$$T(r) = T_1\left[\frac{(1 - r/R_2)}{(1 - R_1/R_2)}\right]^{2/5} ,$$

where $T_1 = T(R_1{}^+)$. Thus, assuming uniform pressure in region (b), equation (57) can be approximated by

$$L_b \propto \frac{R_2^3}{R_1^4}\left(1 - \frac{R_1}{R_2}\right)\frac{1}{T_1^{5/2}}\int_0^{T_1}\frac{dT}{T^{1/2}} \times \left[1 - \left(\frac{T}{T_1}\right)^{5/2}\left(1 - \frac{R_1}{R_2}\right)\right]^2 \Lambda(T) .$$

As long as the ratio R_1/R_2 does not approach unity and $T_1 \gtrsim 10^6$ K, the integral is approximately independent of time. Moreover, the temperature just outside the inner shock, T_1, should scale in the same manner as the mean temperature, $\langle T\rangle$, of region (b). Thus, we assume that $T_1 \propto \langle T\rangle \propto E_b/M_b$, and the functional form for the luminosity used in our calculations is

$$L_b \propto \frac{R_2^3}{R_1^4}\left(\frac{M_b}{E_b}\right)^{5/2}\left(1 - \frac{R_1}{R_2}\right) . \tag{58}$$

This form of the luminosity introduces the additional variable, M_b. The main source of mass to region (b) is the evaporative mass flux due to thermal conduction into the outer shell. The approximate formula for dM_b/dt from Paper I can be improved by using spherical coordinates. For purposes of obtaining an approximate equation for dM_b/dt, we use the following procedure. Assuming stationary flow, the energy flux in region (b) is described by

$$-\frac{1}{4\pi r^2}\frac{dM_b}{dt}\frac{dH}{dr} = \frac{1}{r^2}\frac{d}{dr}\left(r^2 C T^{5/2}\frac{dT}{dr}\right) - n_e n \Lambda(T) , \tag{59}$$

where $H = 5kT/2\mu$ is the specific enthalpy (cf. eq. [5] of Paper I). If the radiative loss term $n_e n\Lambda(T)$ is ignored, integration of equation (59) gives results for dM_b/dt which can be represented by the interpolation formula

$$\frac{dM_b}{dt} = C_1\langle T\rangle^{5/2} R_2^2/(R_2 - R_1) , \tag{60}$$

where the $C_1 = 16\pi\mu C/25k = 1.81 \times 10^{-14}$ (cgs). A better estimate, $C_1 = 4.13 \times 10^{-14}$ (cgs), which incorporates the effects of the nonstationary flow, is obtained by comparison of equation (60) with equation (33). When the radiative losses of region (b) are included, dM_b/dt must decrease. One sees from equation (59) that dimensionally the reduction in dM_b/dt must be proportional to $\mu L_b/kT$. The constant of

proportionality is determined in the following way. We obtain the value of dM_b/dt and L_b from the initial detailed model. Then we solve a modified equation (60) for this constant, C_2:

$$\frac{dM_b}{dt} = C_1\langle T\rangle^{5/2}\frac{R_2^2}{R_2 - R_1} - C_2\frac{\mu L_b}{kT'}, \qquad (61)$$

where $T' = 2 \times 10^5$ K is approximately the temperature at which the time-dependent cooling curve peaks. We find that $C_2 = 2.00$.

Now, equations (58) and (61) together with the evolutionary equations form a closed system of ordinary differential equations that can easily be integrated numerically to find R_1, R_2, V_2, E_b, and M_b as a function of time.

The procedure we have adopted to find the evolution of an interstellar bubble is the following. At some initial time, $t_0 = 5 \times 10^4$ yr, we obtain a detailed model of the interior structure of a bubble. The initial conditions needed for this detailed model are given by the similarity solution. The luminosity of region (b) calculated for this model is used as the coefficient of equation (55). The initial similarity values for R_2, V_2, and E_b and the mass of region (b) calculated for this model from the initial conditions needed to integrate the evolutionary equations. At some new epoch, the resulting variables are then used in similarity-type equations, as discussed in § III*a*. The luminosity calculated from the detailed model at this new epoch, $L_b^{\rm calc}$, is then compared with the value $L_b^{\rm pred}$, predicted by equation (58); if satisfactory agreement is found, the magnitude of the luminosity in equation (58) is adjusted and the evolution continued. If the agreement is not satisfactory [i.e., if $|(L_b^{\rm pred} - L_b^{\rm calc})/L_b^{\rm pred}| > 0.2$], then the time step is reduced until $L_b^{\rm calc}$ varies from $L_b^{\rm pred}$ by less than 20%. In practice we found that with this method we could follow very efficiently the evolution of a bubble.

b) Results

The evolution of the parameters of a typical bubble is shown in Figure 6. The values shown by the solid curves were calculated by assuming that the pressure outside the shell was negligible. The dashed curves show the modifications to these curves if the exterior region is an H II region with $T = 8000$ K. It can be seen that the outer shock varies approximately as $R_2(t) \propto t^{0.58}$, while the inner shock radius varies as $R_1(t) \propto t^{0.44}$. Thus, $R_2(t)$ is overestimated and $R_1(t)$ is underestimated by the simple similarity solution of Paper I. The velocity $V_2(t)$ is slightly less than the approximate result from equation (52), until $V_2(t) \lesssim 10$ km s^{-1}. At this time the exterior pressure becomes important and causes the outer shell to stall at 5×10^6 yr.

The actual energy and mass of region (b) are also reduced from their similarity values. The energy, E_b, at any epoch is reduced by an amount approximately equal to the sum of the total radiated power from the initial time to that epoch. The mass, M_b, is reduced

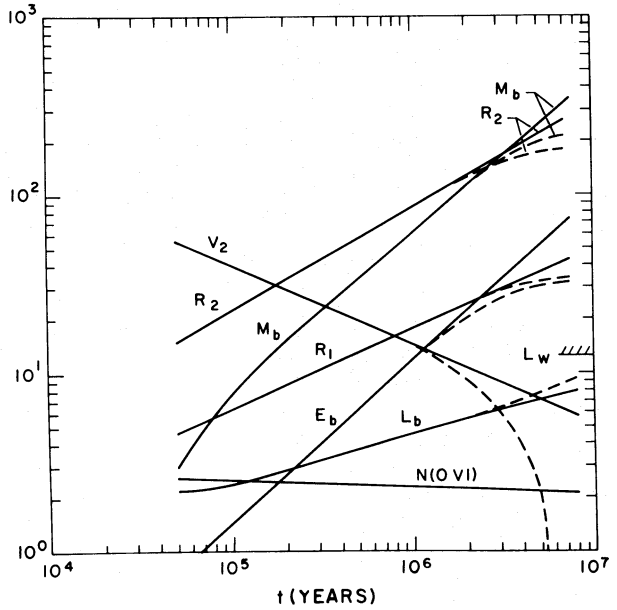

FIG. 6.—The evolution of the important parameters of a bubble for $L_w = 1.27 \times 10^{36}$ and $n_0 = 1$ cm^{-3}. The values shown by the solid curves were calculated by assuming that the pressure outside the outer shell was negligible. The dashed curves show the modifications to these curves if the exterior region is an H II region at $T = 8000$ K. The units of the ordinate are, respectively: R_1, $R_2(10^{18}$ cm); $M_b(10^{33}$ g); $E_b(10^{49}$ ergs); $L_b(10^{35}$ ergs s^{-1}); N(O VI) (10^{13} cm^{-2}); and V_2 (km s^{-1}).

owing to the fact that a large fraction of the thermal energy that is conducted into the shell is radiated away instead of causing evaporation. The actual values of these parameters depend on the asymptotic form of $L_b(t)$ as t becomes large (more than a few times 10^6 yr). We find that L_b never exceeds L_w. This is due to a thermostatic mechanism inherent in the evolution of a bubble. As the radiated power increases, the mass flux into region (b) through the conduction front decreases rapidly (see eq. [61]). The decrease in mass flux across the front causes the density of region (b) to decrease in such a way as to limit any further increase in L_b. Thus the power radiated from this region asymptotically approaches a constant value of some fixed fraction of the wind power, L_w. For the model at $t = 10^6$ yr described in § IV, $L_b \approx 0.4L_w$ and L_b approaches the constant value of $0.9L_w$ as $t \gtrsim 1 \times 10^7$ yr (if the star exists this long). Thus region (b) does not collapse. However, when L_b has to be included in the calculations, one sees from Figure 6 that the expansion of the bubble, $R_2(t) \propto t^{0.58}$, is intermediate between the law $R_2(t) \propto t^{0.60}$ of Paper I and the law $R_2(t) \propto t^{0.5}$ of Steigman, Strittmatter, and Williams (1975).

The increase of the radiated power of region (b) has an interesting effect on the column density of highly ionized species which exist at temperatures $10^4 \leq T \lesssim 10^6$ K. As stated in § V*a*, the physical effect of an increasing luminosity with time is to steepen the temperature gradient in the conduction front. This effect

will tend to decrease the physical radius over which any particular ion is important. However, the volume expansion of the bubble is almost sufficient to equalize this effect. Thus the column density of O VI, for example, varies by only $\sim 15\%$ during the evolution of a bubble. The calculated time variation of N(O VI) is shown in Figure 6. The column density of O VI actually decreases slightly with time, as opposed to the Paper I result that $N(\text{O VI}) \propto t^{8/35}$. So, in this idealized model, the column density of highly ionized species will not be appreciably altered until the early-type star evolves off the main sequence or the wind stops, whichever occurs first.

We have investigated the effect on N(O VI) of reducing the luminosity L_w. The extremely weak dependence of N(O VI) on L_w given by equation (50) is likely to break down for sufficiently small luminosities, and it is important to determine whether this would imply an absence of O VI in stars with weak winds, contrary to observation. A sequence of detailed models having reduced values of L_w shows that equation (50) is obeyed rather well until L_w is reduced to the point that the temperature in the bubble interior, which also declines as L_w is reduced, drops below the values for which O VI is abundant. Further reduction of L_w then decreases N(O VI) sharply. The cutoff value of L_w increases with the age of the bubble, since the bubble temperature *decreases* with age, and at an age of 10^6 yr the cutoff comes at $L_w \approx 2 \times 10^{33}$ ergs s^{-1}. This is consistent with the presence of O VI in essentially all the hot stars that have been observed. The details of these calculations are given by Weaver (1977).

c) *Stability Considerations*

In the idealized model of the bubble we have been discussing up to now, we have assumed that the stellar wind has been blowing with constant luminosity L_w since time $t = 0$ into a medium of uniform density ρ_0. We find in this case that $d^2R_2/dt^2 < 0$. Under such circumstances the system is stably stratified because the hot, low-density gas in the interior of the shell rests "on top" of the dense expanding shell in the sense that a comoving parcel of fluid feels an effective outward gravity. However, if the system is expanding into a gas whose density is decreasing with radius, or if L_w is increasing with time, it is possible that the shell may begin to accelerate. If so, the system should suffer the Rayleigh-Taylor instability and the shell should break into filaments in a time scale comparable with the expansion time scale. Therefore, if the expansion of the shell can be described at any moment by a power law $R(t) \propto t^{\alpha}$, the stability criterion as stated above is $\alpha < 1$.

In order to examine the effect of an unsteady stellar wind and a nonuniform ambient density on the stability of the system, we make a simple dimensional argument to estimate the behavior of $R(t)$ in the more general case where it is assumed that the wind luminosity obeys the law $L_w(t) = K_w t^m$ and the ambient density profile is given by $\rho(r) = K_\rho r^{-n}$. Then it is easy to show that the only quantity with the dimensions of length that one can construct from $L_w(t)$, $\rho(r)$, and t is

$$R(t) = CK_\rho^{-1/(5-n)} K_w^{1/(5-n)} t^{(3+m)/(5-n)}, \quad (62)$$

where C is a dimensionless constant. For example, in the case where $n = m = 0$, so that $K_\rho = \rho_0$ and $K_w = L_w$, we recover the result of Paper I, in which a detailed calculation gives $R(t) = 0.76 L_w^{1/5} \rho_0^{-1/5} t^{3/5}$. We can now write the stability criterion $\alpha < 1$ for the general case in the form

$$n + m < 2. \quad (63)$$

Of course, including the radiative losses L_b in the theory, as we have done in § V*a*, introduces an additional dimensional variable into the system, and this precludes deriving the exponent α in such a simple way. However, since we have found from our detailed studies of the case $n = m = 0$ that the modification of α due to the inclusion of L_b is slight, we think that equation (63) is likely to be a good approximate stability criterion in general.

The development of a Rayleigh-Taylor instability during the expansion of a bubble is likely to occur commonly, because early-type stars must have been born in a high-density molecular cloud and they cannot have moved far from this coeval cloud in their short lifetimes. A newly born star or OB association should begin to blow a bubble while it is inside that cloud. But when $R_2(t)$ reaches the outer boundary of the cloud where the density is decreasing abruptly, the bubble should burst and the circumstellar shell should break up into high-velocity filaments. Then a new bubble of greater size should begin to form in the low-density gas outside the molecular cloud. We suggest that the high-velocity filaments around the Trapezium stars may be the remnant of a bubble that has recently burst.

d) *Effect of Stellar Motion*

Another idealization of our model has been to assume that the star is at rest with respect to its ambient interstellar gas. This is probably a good approximation for the average OB star (Conti, Leep, and Lorre 1977). However, if a particular early-type star has a large space velocity, V_*, then the idealized structure of a bubble will be modified. Therefore we consider briefly these modifications if the star is in uniform motion through a medium of constant density.

Consider first early times, such that $V_* t < R_2(t) - R_1(t)$ where $R_1(t)$ and $R_2(t)$ are the radii of the inner and outer shocks, respectively, calculated as before under the assumption $V_* = 0$. Neglecting $R_1(t)$, and using the approximate theory of Paper I for $R_2(t)$, we may write this condition as

$$t \lesssim 2 \times 10^6 n_0^{-1/2} L_{36}^{1/2} (V_*/20 \text{ km s}^{-1})^{-5/2} \text{ yr}. \quad (64)$$

In this case, to first approximation, the shell at $R_2(t)$ should still be a sphere centered on the original ($t = 0$) stellar position, and the shock at $R_1(t)$ should still be

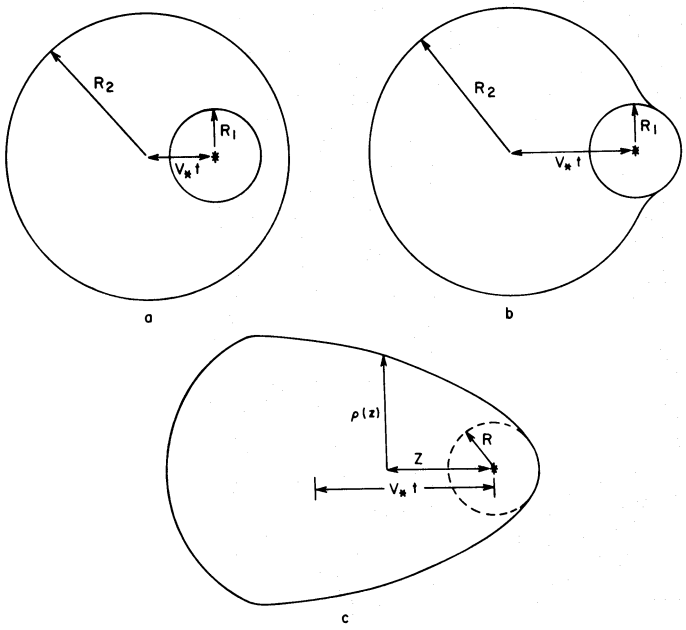

FIG. 7.—Schematic illustration of the effect of stellar motion on the structure of a bubble: (*a*) at early times when $V^*t < R_2 - R_1$; (*b*) at intermediate times for a star that has large velocity with respect to its ambient interstellar medium; (*c*) at extremely advanced times. Note that the scale of this figure changes—i.e., we have kept $R_2(t) \approx$ constant.

a sphere centered on the present ($t = t$) stellar position, as indicated schematically in Figure 7*a*. This approximate description is good for the following reasons. Provided $V_* < C_b$, where $C_b \approx 100$ km s^{-1} is the sound speed in region (b), region (b) remains isobaric as before, irrespective of the stellar location, because $R_2/C_b < t$. Therefore the expansion velocity $V_2(t)$ is independent of direction and centered on the stellar position at $t = 0$. Provided $V_w > C_b$, the inner shock at $R_1(t)$ is also approximately spherical but centered on the stellar position at t because its location is determined by pressure balance between the gas pressure of region (b) and the ram pressure of the stellar wind, whose isobars are concentric with the star.

Once condition (64) is violated, and the shock at $R_1(t)$ abuts the shell at $R_2(t)$, the bubble becomes distorted as indicated schematically by Figure 7*b*. Now the shape of the leading edge of the bubble is determined by a balance between the ram pressure of the stellar wind and that of the interstellar medium; this shape has been calculated by Baranov, Krasnobaev, and Kulikovskii (1971), Baranov, Krasnobaev, and Ruderman (1976), and Dyson (1975). The frontal shock remains a fixed distance ahead of the moving star from this time on unless the density ρ_0 of the ambient gas changes. We have not attempted to calculate the structure of the gas between the two shocks at the leading edge of such a system, but we expect that the column density of O VI through this structure should be much less than before. However, the shape of the trailing part of the bubble should remain approximately spherical, and the column density of O VI along rays trailing the star should be more or less the same as before.

In the limit when $V_*t \gg R_2(t)$, the frontal shock should still have the shape calculated by Baranov, but the trailing part of the bubble should also become elongated as a result of stellar motion. One can show in this case that the shape of the trailing part of the bubble should be approximately a paraboloid of revolution, as indicated schematically in Figure 7*c*. The perpendicular distance ρ from the axis should be related to the distance z behind the star by

$$\rho(z) = [20L_w/(33\pi\rho_0 V_*^3)]^{1/4} z^{1/2} . \quad (65)$$

However, a real star would probably not last long enough for such a system to develop.

VI. THE OUTER SHELL

a) Hydrodynamic Structure

The mass swept up by a bubble of radius R_2 in a medium of uniform density ρ_0 is $M_s = 4\pi\rho_0 R_2^3/3$. We have seen that only a small fraction of this mass is evaporated into region (b), so most remains in a thin shell, through which the column density is

$$N_s = n_0 R_2/3 . \quad (66)$$

The temperature immediately behind the outer shock at R_2 is elevated to a value $T_2 = 3\mu V_2^2/16k$ appropriate to an adiabatic shock; this temperature rise is indicated by the spike at R_2 in Figure 3. However, radiative cooling in this shocked layer should be rapid, so there should be an abrupt drop in temperature and corresponding rise in density behind the shock. The thickness of the radiative cooling zone behind the shock depends on the state of the ambient gas, but

should be $\lesssim 3n_0^{-1}$ pc in any case (see Cox 1972; McCray, Stein, and Kafatos 1975; Field *et al.* 1968; London, McCray, and Chu 1977). The temperature of the gas in the shell behind this zone should be of order $T_{\rm I} \approx 80$ K if the gas is primarily H I or H_2, and of order $T_{\rm II} \approx 8000$ K if the gas is H II as a result of photoionization by the central star. For simplicity in the ensuing discussion, we shall assume that most of the gas in the shell is isothermal at one of the two above temperatures, and that the isothermal sound speed $C_s = (kT/\mu)^{1/2}$ can be $C_{\rm I} \approx 1$ km s^{-1} if the gas is H I or H_2, or $C_{\rm II} \approx 10$ km s^{-1} if the gas is H II. However, the reader should keep in mind that there may be a significant variation through the shell of temperature, hence C_s, in real situations.

Given these assumptions, we may use the jump condition for an isothermal shock to write the gas density n_s in the shell in terms of the upstream ambient density n_0:

$$n_s = n_0(V_2^2 + C_0^2)/C_s^2 , \tag{67}$$

where C_0 is the isothermal sound speed in the ambient gas. Equation (67) is valid only if $C_0^2 + V_2^2 \gg V_2 C_s$. This condition fails when V_2 approaches C_0; in that case the shock at R_2 will weaken and the approximation that region (c) is thin will also fail, with the result that our treatment of the dynamics is no longer correct.

There should be a slight density gradient in the shell because it is decelerating, so the pressure at the inner boundary of the shell should be less than that at R_2. By integrating the equation of hydrostatic equilibrium through the shell in a comoving frame of reference, we find that the gas pressure P_d at the inner boundary of the shell is related to the pressure p_2 immediately behind R_2 by

$$p_d/p_2 = 1 - \frac{dV_2}{dt}\frac{R_2}{3(V_2^2 + C_0^2)} . \tag{68}$$

For example, if $R_2 \propto t^\alpha$ and $V_2 \gg C_0$, then we find $p_d/p_2 = (4\alpha - 1)/3\alpha$, and for the typical value of $\alpha \approx 0.58$, $p_d/p_2 \approx 0.76$. To justify equation (68), one must verify that the time t_s for sound to travel through the shell is less than the age t of the system. One finds $t_s/t \approx C_s R_2/3V_2 t$; $t_s/t \approx 0.03$ for $C_s \approx 1$ km s^{-1}, and $t_s/t \approx 0.3$ for $C_s \approx 10$ km s^{-1}.

In order not to clutter the equations to follow, we shall ignore this variation of pressure through the shell from now on. It is a simple matter to make the appropriate refinements if the reader wishes results that are accurate to within better than a factor of 2.

b) Ionization Structure

As we have already remarked, the expanding shell may be fully ionized by the central star, or it may have an outer layer of H I and H_2 if the ionization front is trapped in the shell. We now find the criterion for trapping of the ionization front and describe how potentially observable quantities depend on the parameters of the system.

Let S_i be the rate of production of ionizing photons by the central star. A table of S_i as a function of spectral type can be found in the paper by Hollenbach, Chu, and McCray (1976). Assume also, for simplicity, that an H II region has a constant temperature $T_{\rm II} \approx 8000$ K, so that the isothermal sound velocity is $C_{\rm II} \approx 10.5$ km s^{-1}. If the star were embedded in a medium of uniform atomic density n_0, the Strömgren radius R_0 would be given by

$$R_0 = [3S_i/(4\pi\alpha^{(2)})]^{1/3} n_0^{-2/3} \approx 30 S_{48}^{1/3} n_0^{-2/3} \text{ pc} , \tag{69}$$

where $S_{48} \equiv (S_i/10^{48}\text{ s}^{-1})$, and $\alpha^{(2)} = 3.1 \times 10^{-13}$ cm^3 s^{-1} is the rate coefficient for radiative recombination to form excited hydrogen atoms at 8000 K (see Osterbrock 1974). Suppose now that a fully ionized circumstellar shell is expanding within the H II region. If so, the rate at which the shell absorbs ionizing photons is given by

$$S_i' = 4\pi R_2^2 \Delta R \alpha^{(2)} n_s^2 , \tag{70}$$

where ΔR is the thickness of the shell. The condition for the ionization front to be trapped by the shell is $S_i' = S_i$; and using equations (69) and (70), we may write this condition as

$$R_2(t_1)/R_0 = \{1 + [V_2(t_1)/C_{\rm II}]^2\}^{-1/3} , \tag{71}$$

where t_1 is the time at which the ionization front is first trapped within the expanding shell. We may obtain a numerical estimate of when this occurs by using the approximate theory of Paper I for $R_2(t)$ and $V_2(t)$. Then one may derive from equations (51), (52), and (71) the transcendental equation

$$1 + (V_2/C_{\rm II})^2 = 0.18 L_{36}^{-3/2} n_0^{-1/2} S_{48} (V_2/C_{\rm II})^{9/2} , \tag{72}$$

where $L_{36} = L_w/10^{36}$ ergs s^{-1}. For example, one finds for $n_0 = 1$, $L_{36} = 1$, and $S_{48} = 12$, which are reasonable estimates for an O7 III star, that $V_2(t_1)/C_{\rm II} \approx 1.0$, which yields $R_2(t_1)/R_0 \approx 0.79$ and $t_1 \approx 4.7 \times 10^6$ yr.

Before the ionization front is trapped, the column density of H II in the expanding shell is given by equation (66), and the thickness of the shell is given by

$$\Delta R_{\rm II} \approx \frac{R_2}{3(1 + V_2^2/C_{\rm II}^2)} . \tag{73}$$

Therefore the emission measure of the shell looking along a ray through its center is given by

$$\text{EM}_0 \equiv 2n_s^2 \Delta R_{\rm II} = 2(1 + V_2^2/C_{\rm II}^2) n_0 R_2/3 . \tag{74}$$

The shell has a bright rim because of the geometry of the system. The ratio of the maximum surface brightness at the rim of the bubble to that at its center is equal to the ratio of path lengths, and may be written

$$\frac{\text{EM}_{\rm rim}}{\text{EM}_0} = (2R_2/\Delta R_{\rm II})^{1/2} = [6(1 + V_2^2/C_{\rm II}^2)]^{1/2} . \tag{75}$$

Once the ionization front is trapped ($t > t_1$), an outer layer of H I forms in the expanding shell. If there are no other early-type stars nearby, the H II between $R_2(t_1)$ and R_0 should cool and recombine, making a "fossil H II region" which may have interesting observable consequences. For example, the cooling time scale of the gas $\tau_c \approx 10^4 n_e^{-1}$ yr, is less than the recombination time scale, $\tau_R \approx 10^5 n_e^{-1}$ yr by a factor ~ 10 (Schwarz 1973). Therefore, there is a possibility of finding cold ($T \lesssim 100$ K), partially ionized ($n_e/n_H \gtrsim 10^{-2}$) gas outside such a bubble by, say, radio recombination-line observations (see Shaver 1976). Further, the cooling gas in the fossil H II region is thermally unstable and should form small-scale H I condensations of high density (Schwarz, McCray, and Stein 1972). However, after a time $t_2 \approx 1.3 t_1$, the expanding shell should sweep up this fossil H II region and continue into the H I beyond.

Now the H II is confined to the inner layer of the shell. Its column density $N_{II} \equiv n_s \Delta R_{II}$ is determined by equating S_i to S_i' of equation (70). This and equation (67) give a column density

$$N_{II} = \frac{S_i}{4\pi\alpha^{(2)} R_2^2 n_0}\left(\frac{C_{II}^2}{V_2^2 + C_0^2}\right) = 2.7 \times 10^{22} S_{48} n_0^{-1} R_2(\mathrm{pc})^{-2}\left(\frac{C_{II}^2}{V_2^2 + C_0^2}\right), \quad (76)$$

thickness

$$\Delta R_{II} = \frac{N_{II}}{n_s} = 9.0 \times 10^3 S_{48} n_0^{-2} R_2(\mathrm{pc})^{-2}\left(\frac{C_{II}^2}{V_2^2 + C_0^2}\right)^2 \mathrm{pc}, \quad (77)$$

and emission measure

$$\mathrm{EM} = 2 n_s N_{II} = 1.8 \times 10^4 S_{48} R_2(\mathrm{pc})^{-2}\ \mathrm{cm}^{-6}\ \mathrm{pc}. \quad (78)$$

We find for reasonable parameters of the theory presented in this paper that the time when the H II ionization front is trapped in the outer shell is approximately equal to the time when the outer shell stalls. The consequence of this time coincidence is that, after the shell stalls, the various column densities through the shell will remain approximately constant. Thus it is possible that the ionization front (I-front) may never be trapped. Indeed, we find that, for the model presented in § V, the H II I-front is almost trapped. However, the shell stalls just before t_1, and thus the outer shell of that model would remain an H II region. One can show that a rough criterion for trapping of the H II I-front is whether $L_{36}^3 n_0 S_{48}^{-2} \gtrsim 5 \times 10^{-3}$.

We note also that the emission measure through a bubble should be nearly independent of time. Before the I-front is trapped $\mathrm{EM}_0 \approx t^{-1/5}$ (see eq. [74]), until the shell stalls; after this time the emission measure is approximately constant. On the other hand, if the I-front were trapped, the shell would stall soon thereafter; again the emission measure would be approximately constant.

One way the emission measure of the shell can be effectively observed is by measuring absorption lines of excited fine-structure levels of ions such as N II** 1085.7 Å. Morton (1975) shows that

$$N(\mathrm{N\ II}^{**}) = 6.4 \times 10^{11}\ \mathrm{EM}\left(\frac{X_N}{8.7 \times 10^{-5}}\right),$$

where the units of N(N II**) and EM are cm^{-2} and cm^{-6} pc, respectively, and X_N is the abundance of nitrogen.

If the I-front were trapped, then the H I column density through the shell would increase until the shell stalled. Molecular hydrogen would then begin to form. Hollenbach, Chu, and McCray (1976) have discussed the time-dependent formation of H_2 in the shell based on the simple theory of Paper I. We note here that the simple results for $R_2(t)$ and $V_2(t)$ given by equations (51) and (52), respectively, should begin to break down just when the H_2 in the shell is forming. Therefore, the theory of Hollenbach *et al.* should be modified appropriately. However, the qualitative behavior of their results should be correct. The molecules in the shell would be formed in a high-pressure and high-UV photon flux environment. Thus one would expect a significant population of high-j molecules (Jura 1975*a*, *b*; Hollenbach, Chu, and McCray 1976). Equation (29) of Hollenbach *et al.* is valid independent of the assumed gas dynamical model, and can be used to relate the column density of high-j molecules to the total H_2 column density and the radius of the shell.

VII. CONCLUSIONS

The main conclusions of our theoretical picture for interstellar bubbles are the following:

1. The hydrodynamic structure of a bubble at early times can be accurately described by a similarity solution, in much the same manner as is done for supernova remnants. However, compared with the SNR theory, there is a continuous injection of energy into a bubble until the wind stops. Including the radiated luminosity of the hot interior causes significant departures from the approximate similarity solution of Paper I. However, the numerical estimates of Paper I are usually within a factor of 2 of the correct answer.

2. The hot interior region (b) will not collapse owing to the large radiative losses ($L_b \lesssim L_w$). Thus the conduction-dominated interface between the shell of swept-up interstellar gas and the hot region will persist for the duration of the stellar wind. Also, the column densities of highly ionized species such as O VI will not be diminished by more than 15% for the same duration.

3. For a typical bubble with $L_w = 1.27 \times 10^{36}$ ergs s^{-1} and $n_0 = 1\ \mathrm{cm}^{-3}$, $N_{\mathrm{O\ VI}}(t = 10^6) = 2.3 \times 10^{13}$ cm^{-2}, which is just in the range of column densities

observed with the UV spectrometer on the *Copernicus* satellite.

4. The emission measure of an interstellar bubble may be observable.

5. The interpretation of stellar or interstellar medium properties based on the radius of an H II region can be significantly altered by the presence of a bubble.

We think such bubbles have been observed. Take, for example, the Gum nebula, whose properties have been reviewed recently by Reynolds (1976*a*, *b*). There have been several theoretical models of the Gum nebula to account for the observed parameters—radius, $R \approx 125$ pc; velocity, $V_{\rm shell} \approx 20$ km s^{-1}; and an emission measure which varies between 20 cm^{-6} pc and 600 cm^{-6} pc across the visible shell (Reynolds 1976*a*, *b*). These models have included the "fossil Strömgren sphere" model, the evolved H II region model, the supernova remnant (SNR) model, and the interstellar bubble model. Reynolds (1976*b*) has reviewed these models in light of recent observations and has concluded that observations support only the SNR and bubble models. His main argument against the bubble interpretation was the fact that ζ Puppis, the star thought to have blown the bubble, was off-center in the nebula, yet the nebula was still spherical in shape.

We believe the theory presented in this paper supports the bubble interpretation of the Gum nebula. Indeed, the stellar wind from ζ Pup is very strong: $dM_w/dt \approx 7 \times 10^{-6}\, M_\odot$ yr^{-1} (Lamers and Morton 1976) and $V_w \approx 2700$ km s^{-1} (Snow and Morton 1976). Furthermore, the interstellar density in the direction of the Gum nebula is low, $n_0 \approx 0.25$ cm^{-3} (Wallerstein and Silk 1971; Gorenstein, Harnden, and Tucker 1974). Assuming these parameters and an age of $t = 10^6$ yr, we find that the radius and velocity from equations (51) and (52) are $R_2 = 126$ pc and $V_2 = 25$ km s^{-1}. These values agree well with the observed parameters of the nebula. Further support of the bubble model is provided by the observed emission measure through various chords of the nebula. Reynolds (1976*a*) shows the emission measure varying from a minimum of ~ 20 cm^{-6} pc near the center of the nebula to a maximum of ~ 500 cm^{-6} pc near the rim, which agrees well with the values obtained from the formula of § VI.

The fact that ζ Pup is still within the "spherical" nebula is easily explained. A large fraction of the observed "radial" velocity of this Of star is likely to originate from atmospheric motion at levels where the absorption lines are formed (Conti, Leep, and Lorre 1977). Thus the velocity of ζ Pup with respect to its local interstellar medium is likely to be less than 20 km s^{-1}, and the bubble found will still be spherical, as was schematically shown in Figure 7*b*.

There are additional sources of stellar wind luminosity inside the Gum nebula. The B association and γ^2 Vel should contribute a significant amount of energy to the interior of the bubble. The main effect of these additional sources is to increase the pressure in region (b) of the entire bubble complex. There should be small cavities (i.e., $r < R_1$) of free streaming stellar winds around each of the sources.

Other shell structures in the interstellar medium which we believe can also be explained by this theory include the Bubble nebula = NGC 7635 (see Icke 1973) and portions of the 30 Doradus complex (Melnick 1976). Further observations of these and other circumstellar shells around hot stars should be made to help to determine stellar and interstellar properties based on the bubble theory. Perhaps the best observational test of the bubble hypothesis would be to make further UV spectroscopic observations to study correlations in the velocities of lines such as N II** λ1086, which indicates the presence of high-pressure H II regions; $H_2(j = 4, 5)$ Lyman lines, which indicate the presence of high-pressure H I in the vicinity of a strong source of UV photons (see Jura 1975*a*, *b*); and O VI λ1035, which indicates the presence of a gas with temperature $T \approx 2$–5×10^5 K.

This work has been supported in part from National Science Foundation grants AST 75-23590 and AST 76-22032, National Aeronautics and Space Administration grant NSG-7128, and a computing grant from the National Center for Atmospheric Research. One of us (R. Moore) has been partially supported by the Energy Research and Development Administration under contract E(11-1)-2887.

REFERENCES

Aldrovandi, S. M. V., and Pequignot, D. 1973, *Astr. Ap.*, **25**, 137; erratum, **47**, 321.
Avedisova, V. S. 1972, *Soviet Astr.—AJ*, **15**, 708.
Baranov, V. B., Krasnobaev, K. V., and Kulikovskii, A. G. 1971, *Soviet Phys. Doklady*, **15**, 791.
Baranov, V. B., Krasnobaev, K. V., and Ruderman, M. S. 1976, *Ap. Space Sci.*, **41**, 481.
Burstein, P., Borken, R. J., Kraushaar, W. L., and Sanders, W. T. 1977, *Ap. J.*, **213**, 405.
Castor, J., McCray, R., and Weaver, R. 1975, *Ap. J.* (*Letters*), **200**, L107 (Paper I).
Conti, P. S., Leep, E. M., and Lorre, J. J. 1977, *Ap. J.*, **214**, 759.
Cowie, L., and McKee, C. 1977, *Ap. J.*, **211**, 135.
Cox, D. P. 1970, Ph.D. thesis, University of California at San Diego.
———. 1972, *Ap. J.*, **178**, 143, 159.
Cox, D. P., and Tucker, W. H. 1969, *Ap. J.*, **157**, 1157.
den Boggende, A. J. F., Mewe, R., Heise, J., Gronenschild, E. H. B. M., and Grindlay, J. 1977, *Astr. Ap.*, in press.
Dyson, J. E. 1975, *Ap. Space Sci.*, **35**, 299.
Falle, S. A. E. G. 1975, *Astr. Ap.*, **43**, 323.
Field, G. B., Rather, J. D. G., Aannestadt, P. A., and Orszag, S. A. 1968, *Ap. J.*, **151**, 953.
Gorenstein, P., Harnden, F. R., Jr., and Tucker, W. H. 1974, *Ap. J.*, **192**, 661.
Hollenbach, D., Chu, S.-I., and McCray, R. 1976, *Ap. J.*, **208**, 458.
Holzer, T. E., and Axford, W. I. 1970, *Ann. Rev. Astr. Ap.*, **8**, 31.
Icke, V. 1973, *Astr. Ap.*, **26**, 45.
Jenkins, E. B., and Meloy, D. A. 1974, *Ap. J.* (*Letters*), **193**, L121.
Jura, M. 1975*a*, *Ap. J.*, **197**, 575.
———. 1975*b*, *Ap. J.*, **197**, 581.

Lamers, H. J., and Morton, D. C. 1976, *Ap. J. Suppl.*, **32**, 715.
London, R., McCray, R., and Chu, S.-I. 1977, *Ap. J.*, in press.
McCray, R., Stein, R., and Kafatos, M. 1975, *Ap. J.*, **196**, 565.
Melnick, J. 1976, Ph.D. thesis, California Institute of Technology.
Morton, D. C. 1975, *Ap. J.*, **197**, 85.
Osterbrock, D. E. 1974, *Astrophysics of Gaseous Nebulae* (San Francisco: Freeman).
Reynolds, R. J. 1976*a*, *Ap. J.*, **203**, 159.
———. 1976*b*, *Ap. J.*, **206**, 679.
Schwarz, J. 1973, *Ap. J.*, **182**, 449.
Schwarz, J., McCray, R., and Stein, R. 1972, *Ap. J.*, **175**, 673.
Shapiro, P. R., and Moore, R. 1976, *Ap. J.*, **207**, 460.
Shaver, P. A. 1976, *Astr. Ap.*, **49**, 1.
Snow, T. P., and Morton, D. C. 1976, *Ap. J. Suppl.*, **32**, 429.
Spitzer, L., Jr. 1962, *Physics of Fully Ionized Gases* (New York: Interscience).
Steigman, G., Strittmatter, P. A., and Williams, R. E. 1975, *Ap. J.*, **198**, 575.
Taylor, G. 1950, *Proc. Roy. Soc. London, A*, **201**, 159.
Tidman, D. A., and Krall, N. A. 1971, *Shock Waves in Collisionless Plasmas* (New York: Wiley-Interscience).
Tucker, W., and Koren, M. 1971, *Ap. J.*, **168**, 283.
Wallerstein, G., and Silk, J. 1971, *Ap. J.*, **170**, 289.
Weaver, R. 1977, Ph.D. thesis, University of Colorado.
York, D. G. 1974, *Ap. J.* (*Letters*), **193**, L127.
Zel'dovich, Ya. B., and Raizer, Yu. P. 1967, *Physics of Shock Waves and High Temperature Hydrodynamic Phenomena* (New York: Academic Press).

JOHN CASTOR and RICHARD MCCRAY: Joint Institute for Laboratory Astrophysics, University of Colorado, Boulder, CO 80309

ROBERT MOORE and PAUL SHAPIRO: Center for Astrophysics, 60 Garden Street, Cambridge, MA 02138

ROBERT WEAVER: Code 660, NASA/Goddard Space Flight Center, Greenbelt, MD 20771